Open access • Journal Article • DOI:10.1103/PHYSREVLETT.93.083904

# Kerr-nonlinearity optical parametric oscillation in an ultrahigh-Q toroid microcavity



Tobias J. Kippenberg, Sean M. Spillane, Kerry J. Vahala

**Institutions:** California Institute of Technology

**Published on:** 19 Aug 2004 - Physical Review Letters (American Physical Society)

**Topics:** Optical parametric amplifier, Optical microcavity, Toroid, Kerr effect and Nonlinear optics

# Kerr-Nonlinearity Optical Parametric Oscillation in an Ultrahigh-$Q$ Toroid Microcavity

T. J. Kippenberg, S. M. Spillane, and K. J. Vahala*

*California Institute of Technology, Thomas J. Watson Laboratory of Applied Physics, Pasadena, California 91125, USA*

(Received 29 January 2004; published 19 August 2004)

Kerr-nonlinearity induced optical parametric oscillation in a microcavity is reported for the first time. Geometrical control of toroid microcavities enables a transition from stimulated Raman to optical parametric-oscillation regimes. Optical parametric oscillation is observed at record low threshold levels (174 micro-Watts of launched power) more than 2 orders of magnitude lower than for optical-fiber-based optical parametric oscillation. In addition to their microscopic size (typically tens of microns), these oscillators are wafer based, exhibit high conversion efficiency (36%), and are operating in a highly ideal "two photon" emission regime, with near-unity ($0.97 \pm 0.03$) idler-to-signal ratio.

DOI: 10.1103/PhysRevLett.93.083904 PACS numbers: 42.65.Yj, 42.55.Sa, 42.65.Hw

Optical parametric oscillators (OPOs) rely on energy and momentum conserving optical processes to generate light at new "signal" and "idler" frequencies. In contrast to oscillation based on stimulated gain, optical parametric oscillation does not involve coupling to a dissipative reservoir. The lack of such dissipation makes them uniquely suited for fundamental studies, such as the generation of nonclassical states [1,2] for quantum information research [3] as well as in numerous applied areas (e.g., photonics, spectroscopy, sensing). However, oscillation based on optical parametric gain requires stringent phase matching of the involved optical fields [4]. This combined with the necessity of high field intensity or long interaction length poses severe challenges to attaining microcavity optical parametric oscillators. In fact, whereas microcavity stimulated nonlinear oscillators have been demonstrated [5–9], optical parametric equivalents have not been demonstrated so far.

Here we report Kerr-nonlinearity induced optical parametric oscillation in a toroidal microcavity. Toroid microcavities are silica-based whispering-gallery-type resonators possessing ultrahigh $Q$ factors [10]. Efficient coupling, with high ideality [11] is achieved using tapered optical fibers [12] as coupling elements. While ultrahigh-$Q$ ensures high circulating field intensities within the resonator [13], causing a variety of nonlinear optical effects [5–7,9,14], it is not a sufficient condition to ensure parametric oscillation. Because of inversion symmetry, the lowest order nonlinearity in silica is the third order nonlinearity so that the elemental parametric interaction converts two pump photons ($\omega_p$) into signal ($\omega_S$) and idler ($\omega_I$) photons [2,4]. In order for parametric oscillations to occur, both energy and momentum must be conserved in this process [4,15]. In whispering-gallery-type resonators, such as microtoroids, momentum is intrinsically conserved when signal and idler angular mode numbers ($\ell$) are symmetrically located with respect to the pump mode (i.e., $\ell_{S,I} = \ell_p \pm N$) [16]. Energy conservation ($2\omega_p = \omega_S + \omega_I$), on the other hand, is not expected to be satisfied *a priori,* since the resonant frequencies are, in general, irregularly spaced due to both cavity and material dispersion. As a result, the parametric gain is a function of the frequency detuning $\Delta\omega = 2\omega_p - \omega_S - \omega_I$, which effectively gives the degree to which the cavity modes violate strict energy conservation. It can be shown that the existence of parametric gain requires that this detuning be less than the parametric gain bandwidth [15] $\Omega = 4\frac{c}{n}\gamma P$ ($\gamma = \frac{\omega}{c}\frac{n_2}{A_{\text{eff}}}$) where $n_2 \approx 2.2 \times 10^{-20}\ \frac{\text{m}^2}{\text{W}}$ is the Kerr nonlinearity for silica [4] and $P$ is the circulating power within the microcavity. The parametric bandwidth $\Omega$ can be understood by self- and cross-phase modulations, which effectively pull the cavity modes into resonance.

By equating parametric gain and microcavity loss (as determined by the loaded $Q$ factor), the threshold pump power necessary in the waveguide is obtained for parametric oscillation.

$$P_t^{\text{Kerr}} = \frac{\omega_0^2 Q_0^{-2}(1+K)^2 + (\Delta\omega/2)^2}{\gamma\Delta\omega\frac{c}{n_{\text{eff}}}}\ \frac{C(\Gamma)\pi^2 R n_{\text{eff}}}{2\lambda_0} \times \frac{(K+1)^2}{Q_0 K}.$$

Here $K \equiv Q_0/Q_{ex}$ characterizes the coupling of the resonator to a waveguide used for both pumping of the resonator and collection of oscillator power. This coupling is characterized as overcoupled ($K > 1$), critical ($K = 1$), and undercoupled ($K < 1$) using the standard definitions [17]. $Q_0$ and $Q_{ex}$ are the intrinsic and the external (coupling related) quality factors, respectively. $R$ is the principal cavity radius, $n_{\text{eff}}$ is the effective index, $c$ is the speed of light in vacuum, and $C(\Gamma)$ is a correction factor in the range of $[1 \ldots 2]$ taking into account the reduction of circulating power in the presence of modal coupling of the degenerate clockwise and counterclockwise "whispering-gallery modes" (WGMs) [18]. Figure 1 shows both parametric and Raman oscillation regimes as a function of the detuning frequency $\Delta\omega$ and the cou-

  

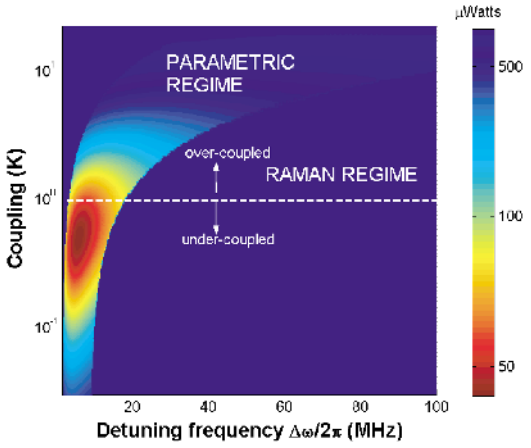


FIG. 1 (color). Nonlinear processes in a microcavity with $D = 50\ \mu$m, $d = 4\ \mu$m, and $Q_0 = 10^8$. The vertical axis denotes coupling strength $K$ of the waveguide-resonator system while the horizontal axis denotes frequency detuning. The dotted line corresponds to the critical coupling point (defined by vanishing waveguide transmission [17,21]). The dark blue colored part of the spectrum denotes areas where Raman oscillation occurs. The color-coded region corresponds to the parametric-oscillation regime (where the parametric threshold is indicated by color in $\mu$W).

pling parameter $K$. The threshold pump power for parametric oscillation is color coded as indicated. As stimulated Raman scattering does not depend on the detuning frequency (i.e., it is intrinsically phase matched), it is the dominant nonlinear mechanism by which light is generated for large detuning values. With decreasing $\Delta\omega$, a transition from stimulated to parametric regimes occurs when the threshold for parametric oscillation falls below that for Raman. (The peak parametric gain is larger than the peak Raman gain, $g_{\mathrm{Kerr}}^{\max} \approx 2g_R^{\max}$ [4].) Also note that for increased waveguide loading (and hence correspondingly higher threshold pump powers) the transition can be made to occur for detuning values that are progressively larger.

To bring about the condition $0 < \Delta\omega < \Omega$ a reduction of the toroidal cross-sectional area reduces the modal effective area $A_{\mathrm{eff}}$ [19] and produces a twofold benefit. First, it increases the parametric bandwidth $\Omega$ through its dependence on $\gamma$ , and second, it reduces $\Delta\omega$. The latter occurs because of increased modal overlap with the surrounding dielectric medium (air) and hence flattening of the modal dispersion. Numerical finite-element modeling was used to calculate the dependence of $A_{\mathrm{eff}}$ on the toroid principal ($D$) and minor diameter ($d$). Figure 2 shows the calculated modal area for a fundamental toroidal WGM as the dotted and solid lines (TE and TM polarization). Note that the case ($d = D$) corresponds to a spherical microcavity. Thus, the desired transition can be induced with toroidal geometries of high principal-to-minor toroid diameter (high aspect ratio), where the principal diameter ($D$) denotes the outer cavity diameter and the minor diameter ($d$) refers to the smaller, toroid cross-sectional diameter (see inset of Fig. 2).

In order to confirm this prediction, toroid microcavities with an approximately constant principal diameter ($D$) and varying minor diameter ($d$) in the range of 3.8–10 $\mu$m were fabricated. Because of the ultrahigh $Q$ of the toroidal WGMs, ultralow-threshold, stimulated Raman scattering was consistently observed for toroids having an aspect ratio of ca. $D/d < 15$ [20]. For microtoroids having an aspect ratio ($D/d$) in excess of ca. 15 a transition (and a subsequent quenching of Raman) to parametric oscillation was observed. Figure 3 shows a parametric-oscillation emission spectra for a microtoroid with $d = 3.9\ \mu$m, $D = 67\ \mu$m, and $Q_0 = 0.5 \times 10^8$. In this measurement a single fundamental WGM of a microtoroid is pumped in the telecommunication window near 1550 nm using tapered optical-fiber waveguides [12,21]. Phase matching of taper mode and WGM was achieved by varying the taper waist in the coupling region. In this way high ideality of the coupling junction was achieved [11]. The parametric interaction in the microcavity causes emission of copropagating signal and idler modes, which are coupled into the forward direction of the tapered fiber. Some residual signal and idler reflection was detected in the backward direction due to the presence of modal coupling [18], induced by backscattering. The generated signal and idler modes had identical oscillation threshold, within the experimental resolution set primarily by taper coupling variations (ca. $\pm 5\%$). Figure 4 shows the parametric-oscillation thresh-

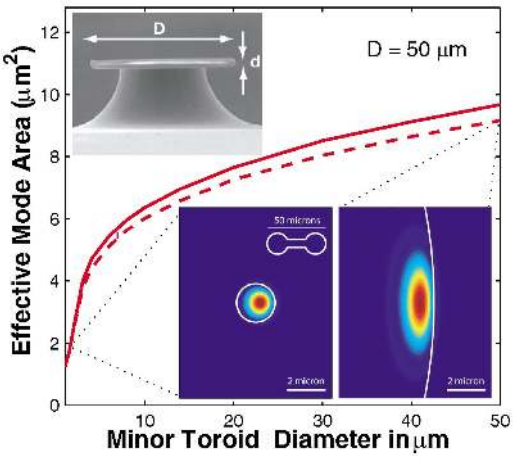


FIG. 2 (color). Calculated effective WGM mode area [19] as a function of minor toroid diameter (for a fixed principal diameter $D = 50\ \mu$m). The solid and dotted lines are the mode area obtained from finite-element modeling of the fundamental toroidal WGM (dotted line: TE polarization; solid line: TM polarization) at a wavelength of 1550 nm. For comparison the inset shows modeled field intensity plots of a fundamental microsphere WGM (right panel) and a toroid WGM of equal principal diameter and $d = 2\ \mu$m (left panel). Upper inset: Scanning-electron micrograph of a toroid microcavity with the geometry parameters indicated.

old as a function of the taper-toroid coupling gap for the toroid microcavity of Fig. 3. Analysis of the threshold equation shows that the coupling point of minimum threshold is a function of the detuning frequency. At the optimum frequency detuning (i.e., maximum parametric gain, for $\Delta\omega_{\mathrm{opt}} = 3\frac{\omega}{Q_0}$), the minimum threshold occurs undercoupled for $K_{\mathrm{min}} = 0.5$ with finite pump transmission ($T_{\mathrm{min}} = 1/9$), whereas for larger detuning the minimum threshold point shifts towards being overcoupled (compare Fig. 1). The measured minimum threshold in the present case was 339 $\mu$W and occurred for the taper displaced by 0.04 $\mu$m into the undercoupled regime. The corresponding pump transmission was $T = (\frac{1-K}{1+K})^2 \approx 4\%$ ($\longrightarrow K \approx 0.67$), indicating that the frequency detuning is close to being optimum. Above threshold the signal and idler fields increase approximately linearly with pump power (for high pump power $P$, the emission scales $P_{S,I} \propto \sqrt{P} - \sqrt{P_t}$). The inset of Fig. 3 shows a pump-to-idler conversion characteristic at the point of minimum threshold. The corresponding differential conversion efficiency was 17% pump to idler. (The total differential conversion efficiency of pump to both signal and idler fields was 34%.) Comparison of the differential conversion efficiency to theory $\eta = 2(1 + K^{-1})^{-2}$ is consistent with the minimum threshold occurring undercoupled, as the inferred coupling point is $K = 0.7$ (corresponding to $T = 4\%$ in agreement with the above measured value). Using the minimum threshold data and the cavity ring-down measurements a detuning frequency of $\Delta\omega/2\pi \approx 24$ MHz is inferred from the threshold equation, compared with $\Delta\omega_{\mathrm{opt}}/2\pi = 11.6$ MHz for the optimum detuning frequency at the measured $Q$ value. The lowest measured parametric-oscillation threshold for the microtoroids in this study was 170 $\mu$W of launched power in the fiber (for a microcavity with $D/d = 16$, $d = 4$ $\mu$m, $Q_0 = 1.25 \times 10^8$, and $\Delta\omega/2\pi \approx 18$ MHz) and is a factor of 200 lower than for fiber OPOs [22] that utilize the dispersion control provided by photonic crystal fiber [23]. As a further confirmation that parametric oscillation is present, both signal and idler emission were recorded for varying pump power. From theory a signal-to-idler photon creation ratio of unity is expected for parametric oscillation [4]. The inset of Fig. 3 shows the measured idler emission power plotted versus signal emission power through the optical-fiber taper. The recorded data were corrected for modal coupling [18] by measuring the reflected power for all three resonances at the critical point. After correcting for modal coupling, the ratio of idler conversion to signal conversion was $0.97 \pm 0.03$. The observation of near-unity idler-signal emission-power ratio, along with the identical threshold for signal and idler wave emission, demonstrates that the observed emission bands can solely be attributed to Kerr-induced microcavity parametric oscillation. Finally, stimulated Brillouin scattering (SBS) was not present, despite having a nearly 3 orders of magnitude larger gain in comparison to the parametric gain. As noted previously, SBS is unlikely to occur in

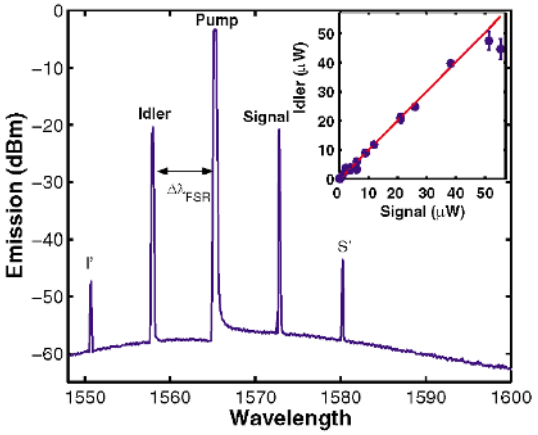


FIG. 3 (color). Parametric oscillation spectrum measured for a 67-$\mu$m-diameter toroidal microcavity. The pump is located at 1565 nm and power levels are far above threshold. The signal and idler are modes with successive angular mode numbers and are spaced by twice the free spectral range ($2 \times 7.6$ nm). The subsidiary peaks (denoted $I'$, $S'$) appeared only at high pump powers and are due to a combination of nonlinear effects, such as parametric oscillation (of signal and idler), as well as four-wave mixing involving the idler, pump, and signal. Inset: idler emission power plotted versus the signal emission power, recorded for different pump powers. The idler-to-signal power ratio is $0.97 \pm 0.03$. For higher pump powers deviation is observed due to the appearance of secondary oscillation peaks ($I'$, $S'$) (compare main figure).

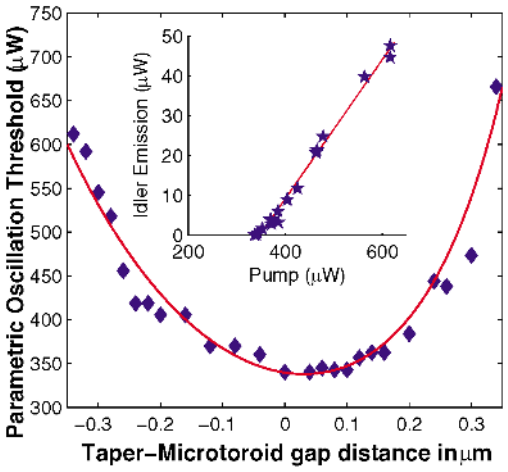


FIG. 4 (color). The coupling-gap dependence of the parametric threshold with respect to the critical coupling point measured using a 67-$\mu$m-diameter toroid microcavity. The minimum threshold occurs with the tapered optical fiber 0.04 $\mu$m undercoupled (with finite transmission of ca. 4%). The solid line is a theoretical fit using the threshold equation. Inset: Idler emission versus pump power. The differential conversion efficiency from pump to idler was 17% (and correspondingly 34% for pump to signal and idler).

microcavities [8], in particular, as microtoroids exhibit a strongly reduced mode spectrum due to azimuthal confinement [10,20], making overlap with the gain bandwidth of SBS unlikely.

We have thus observed for the first time (to the authors' knowledge) Kerr-nonlinearity induced optical parametric oscillation in a microcavity. Parametric interactions provide a distinct and important class of nonlinearity in both applied (nonlinear optics, photonics, spectroscopy) and fundamental areas (quantum optics and quantum information science), and as such this result should extend the range of microcavity applications into new fields. In addition to the highly advantageous practical aspects of on-chip microcavity nonlinear oscillators (such as wafer-scale integration and control), these oscillators exhibit important properties due to the nature of the underlying nonlinear process within the microcavity. Specifically, a phase-sensitive amplification process that can exclude competing Brillouin or Raman processes, as demonstrated here, with a highly ideal coupling junction can provide an excellent candidate system for the generation of nonclassical states of light [1,2,24–29] in a microcavity. In particular, parametric interaction, as reported here, is known to produce correlated "twin beams" at the signal and idler frequencies, having intensities that are correlated to below the shot-noise limit, corresponding to the squeezing of the amplitude difference [1,30]. The latter effect seems particularly promising to study in toroid microcavities. The negligible parasitic loss of the coupling junction [11], the direct coupling to an ultralow loss transport medium (optical fiber), and the high modal purity of toroidal microcavities (single transverse mode oscillation) are important prerequisites for both applied and quantum optical studies. Microcavity generation of nonclassical states could be of particular interest in quantum information [3] and quantum optical studies [2,30–32] as well as for novel bio-imaging schemes based on entanglement [33].

This work was funded by the NSF, DARPA, and the Caltech Lee Center for Advanced Networking.

*Note added.*—The authors request the readers' attention to a parametric $LiNbO_3$ device reported by Ilchenko *et al.* [34].

*To whom correspondence should be addressed.
Email address: vahala@its.caltech.edu

[1] D. F. Walls and G. Milburn, *Quantum Optics* (Springer, New York, 1994).
[2] M. Scully and M. Zubairy, *Quantum Optics* (Cambridge University Press, Cambridge, 1996).
[3] D. Bouwmeester, A. Ekert, and A. Zeilinger, *The Physics of Quantum Information* (Springer, Heidelberg, 2000).
[4] R.W. Boyd, *Nonlinear Optics* (Academic Press, Boston, 1992).
[5] A. J. Campillo, J. D. Eversole, and H. B. Lin, Phys. Rev. Lett. **67**, 437 (1991).
[6] R. Chang and A. J. Campillo, *Optical Processes in Microcavities*, Advanced Series in Applied Physics Vol. 3 (World Scientific, Singapore, 1996).
[7] S. X. Qian and R. K. Chang, Phys. Rev. Lett. **56**, 926 (1986).
[8] S. M. Spillane, T. J. Kippenberg, and K. J. Vahala, Nature (London) **415**, 621 (2002).
[9] S. Uetake, M. Katsuragawa, M. Suzuki, and K. Hakuta, Phys. Rev. A **61**, 011803 (2000).
[10] D. K. Armani, T. J. Kippenberg, S. M. Spillane, and K. J. Vahala, Nature (London) **421**, 925 (2003).
[11] S. M. Spillane, T. J. Kippenberg, O. J. Painter, and K. J. Vahala, Phys. Rev. Lett. **91**, 043902 (2003).
[12] J. C. Knight, G. Cheung, F. Jacques, and T. A. Birks, Opt. Lett. **22**, 1129 (1997).
[13] V. B. Braginsky, M. L. Gorodetsky, and V. S. Ilchenko, Phys. Lett. A **137**, 393 (1989).
[14] F. Treussart, V. S. Ilchenko, J. F. Roch, J. Hare, V. Lefevre-Seguin, J. M. Raimond, and S. Haroche, Eur. Phys. J. D **1**, 235 (1998).
[15] R. H. Stolen and J. E. Bjorkholm, IEEE J. Quantum Electron. **18**, 1062 (1982).
[16] In a WG-type microcavity the propagation constant $\beta_m = m/R$, where $m$ is the angular mode number.
[17] H. A. Haus, *Waves and Fields in Optoelectronics* (Prentice-Hall, Englewood Cliffs, NJ, 1984).
[18] T. J. Kippenberg, S. M. Spillane, and K. J. Vahala, Opt. Lett. **27**, 1669 (2002).
[19] For a third order process the effective mode area is defined as $A_{\text{eff}} \equiv (\int |\vec{E}|^2 dA)^2 / \int |\vec{E}|^4 dA$, where $\vec{E}$ is the electric field of the WGM.
[20] T. J. Kippenberg, S. M. Spillane, and K. J. Vahala, Opt. Lett. **29**, 1224 (2004).
[21] M. Cai, O. Painter, and K. J. Vahala, Phys. Rev. Lett. **85**, 74 (2000).
[22] J. E. Sharping, M. Fiorentino, P. Kumar, and R. S. Windeler, Opt. Lett. **27**, 1675 (2002).
[23] P. Russell, Science **299**, 358 (2003).
[24] M. Fiorentino, P. L. Voss, J. E. Sharping, and P. Kumar, IEEE Photonics Technol. Lett. **14**, 983 (2002).
[25] R. M. Shelby, M. D. Levenson, S. H. Perlmutter, R. G. Devoe, and D. F. Walls, Phys. Rev. Lett. **57**, 691 (1986).
[26] C. Silberhorn, P. K. Lam, O. Weiss, F. Konig, N. Korolkova, and G. Leuchs, Phys. Rev. Lett. **86**, 4267 (2001).
[27] A. Sizmann and G. Leuchs, in *Progress in Optics*, Progress in Optics Vol. 39 (North-Holland, Amsterdam, 1999), pp. 373–469.
[28] R. E. Slusher, L.W. Hollberg, B. Yurke, J. C. Mertz, and J. F. Valley, Phys. Rev. Lett. **55**, 2409 (1985).
[29] L. J. Wang, C. K. Hong, and S. R. Friberg, J. Opt. B **3**, 346 (2001).
[30] A. Heidmann, R. J. Horowicz, S. Reynaud, E. Giacobino, C. Fabre, and G. Camy, Phys. Rev. Lett. **59**, 2555 (1987).
[31] E. S. Polzik, J. Carri, and H. J. Kimble, Phys. Rev. Lett. **68**, 3020 (1992).
[32] K. S. Zhang, T. Coudreau, M. Martinelli, A. Maitre, and C. Fabre, Phys. Rev. A **64**, 033815 (2001).
[33] B. E. A. Saleh, B. M. Jost, H. B. Fei, and M. C. Teich, Phys. Rev. Lett. **80**, 3483 (1998).
[34] V. Ilchenko *et al.*, Phys. Rev. Lett. **92**, 043903 (2004).